Sensors

DOI: 10.1002/ange.201306688

Selective and Sensitive Chromofluorogenic Detection of the Sulfite Anion in Water Using Hydrophobic Hybrid Organic–Inorganic Silica Nanoparticles**

Luis Enrique Santos-Figueroa, Cristina Giménez, Alessandro Agostini, Elena Aznar, María D. Marcos, Félix Sancenón, Ramón Martínez-Máñez, and Pedro Amorós*

Nowadays, sulfites or sulfiting agents such as sodium, calcium, and potassium sulfite (SO_3^{2-}); metabisulfite ($S_2O_5^{2-}$); and bisulfites (HSO_3^-) as well as sulfur dioxide (SO_2) are compounds widely used as preservative and antimicrobial agents to prevent browning of foods and beverages (E220–228 additives).[1] However, several studies had associated topical, oral, or parenteral exposure to high doses of sulfite with adverse reactions as dermatitis, urticaria, flushing, hypotension, abdominal pain, and diarrhoea.[2] In fact, several reports confirmed that some people can be extremely sensitive even to very low sulfite levels[3] and that bronchoconstriction can occur in many asthmatic patients[4] or in people exposed to high doses.[5] Exposure to high doses of sulfite can occur for consumption of food and drinks that contain this additive (as fruits, vegetables, salads, meat, gelatine, juices, vinegar, soft drinks, beer, wine, and others), through the use of several drugs (adrenaline, phenylephrine, corticosteroids, and local anaesthetics), some cosmetics (hair colors and bleaches, creams, and perfumes) or in some occupational settings (leather, textile, mineral, pulp, rubber, agriculture, and chemical industries).[2a] The addition of low levels of sulfite (as low as $0.7\,mg\,kg^{-1}$ of body weight dictated by FAO/WHO)[6] are permitted in beer, wine, and some food under rigorous control, but in many countries their addition, especially in fresh products as salads, fruit, mincemeat, or sausages, is prohibited.[1,7]

Sulfur dioxide is an important and very common air pollutant. When SO_2 is dissolved in aqueous media a pH-dependent equilibrium occurs and it favors the formation of sulfite and bisulfite at neutral pH value.[8] Many studies suggested that extended exposition to SO_2 and/or its derivatives could produce different toxicological effects such as cancer, cardiovascular diseases, neurological disorders, and the change of the characteristics of voltage-gated sodium and potassium channels.[9]

Taking into account the above-mentioned facts, the interest in the development of fast and efficient methods for sulfite detection has increased in the last years. In particular, methods based on electrochemistry,[10] spectrophotometry,[11] chromatography,[12] capillary electrophoresis,[13] and titration[8b,14] have been extensively used for the detection and quantification of sulfite. Recently, the development of chromofluorogenic sensors for anion detection has become a field of interest, since they usually offer several advantages in terms of sensitivity, selectivity, and simplicity of operation over classic, nonportable, and expensive instrumental analysis.[15] In spite of these advantages, few chemosensors for the chromofluorogenic detection of the sulfite anion have been described. In this field, specific reactions of sulfite with aldehydes,[16] levulinate esters,[17] Michael-type additions,[18] and coordinative interactions[19] have been recently used. However, some of those reported probes show certain drawbacks such as low sensitivities and selectivities, poor performane in pure water, the need for using acidic environment ($pH < 5.5$), or large response times. Moreover, very recently some chemosensors for sulfite detection with good stability based on the use of carbon quantum dots,[20] gold nanoparticles,[21] and polymers[22] have been reported. In addition, some sulfite biosensors have been described based on the aerobic oxidation of sulfite by immobilized sulfite oxidase and its electrochemical breakdown under high voltage.[23] These biosensors are sensitive even in pure water, however, have generally low stability, significant metabolite interference, short life, and high cost.

We herein report the development of a simple material for the selective and sensitive chromofluorogenic recognition of sulfite in aqueous solution. We have used functionalized MCM-41 nanoparticles containing a suitable sulfite probe within highly hydrophobic mesopores. The structure of the used organic probe **2** and the synthetic procedure for the

[*] L. E. Santos-Figueroa, C. Giménez, Dr. A. Agostini, Dr. E. Aznar, Dr. M. D. Marcos, Dr. F. Sancenón, Prof. R. Martínez-Máñez
Instituto de Reconocimiento Molecular y Tecnológico
Centro Mixto Universidad Politécnica de Valencia-Universidad de Valencia (Spain)
and
Departamento de Química, Universidad Politécnica de Valencia
Camino de Vera s/n, 46022 Valencia (Spain)
and
CIBER de Bioingeniería, Biomateriales y Nanomedicina (CIBER-BBN)
E-mail: rmaez@qim.upv.es
Homepage: http://idm.webs.upv.es/
Prof. P. Amorós
Instituto de Ciencia de los Materiales (ICMUV)
Universidad de Valencia (Spain)

[**] Financial support from the Spanish Government (project MAT2012-38429-C04) and the Generalitat Valenciana (project PROMETEO/2009/016) is gratefully acknowledged. We also thank the Fundación Carolina and UPNFM-Honduras for a doctoral grant to L.E. Santos-Figueroa and to the Spanish Ministerio de Ciencia e Innovación for a doctoral grant to C. Giménez.

Supporting information for this article is available on the WWW under http://dx.doi.org/10.1002/anie.201306688.

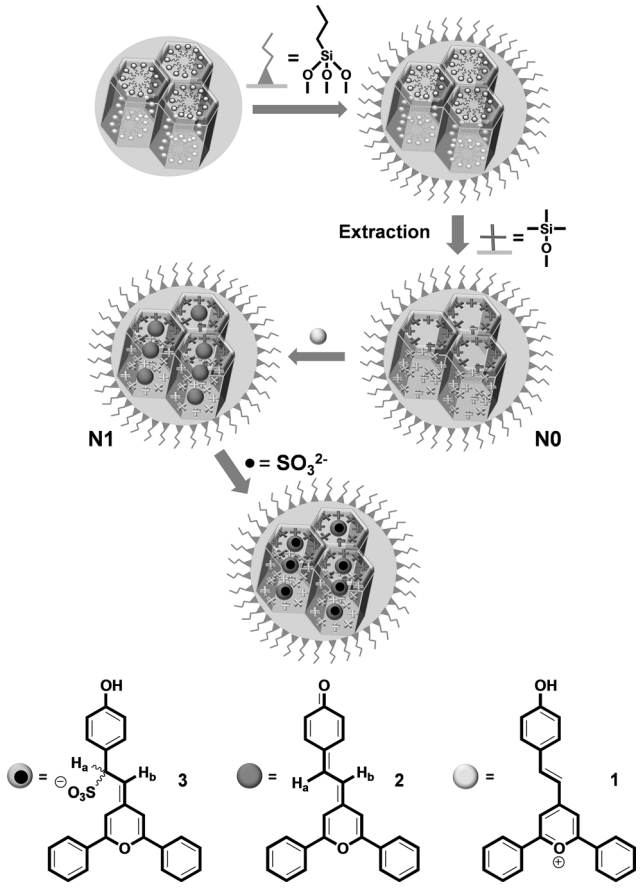

Scheme 1. Representation of the preparation of **N0** nanoparticles, the final sensing material **N1** (with probe **2** located inside the hydrophobic cavities), and proposed chromofluorogenic reaction with sulfite anion.

preparation of the hybrid sensing nanoparticles (**N1**) are shown in Scheme 1.

The design of the probe involves the preparation of a sensing material that should ideally be hydrophobic enough to maintain the probe in the nanopores but not too hydrophobic in order to obtain stable suspensions of the nanoparticles (note that highly hydrophobic nanoparticles tend to float in water, which inhibits fast reaction with the analyte). After several attempts (see the Supporting Information for a detailed discussion) the following procedure was selected for the preparation of **N1**. MCM-41 mesoporous nanoparticles (diameter of ca. 100 nm) were selected as inorganic scaffolds.[24,25] Before the extraction of the cetyltrimethylammonium bromide (CTAB; used as structure-directing agent), the external surface of the silica nanoparticles was functionalized with propyltrimethoxysilane. Then the CTAB located inside the pores was extracted with hydrochloric acid. Finally, the inner sides of the pore walls were hydrophobized with hexamethyldisilazane (see the Supporting Information for details). These experimental procedures yield inorganic nanoparticles (**N0**) containing hydrophobic pockets. The organic content in **N0** was determined by thermogravimetric and elemental analysis and amounts to 0.22 mg of organic matter per mg SiO_2.

The final hybrid nanoparticles **N1** were prepared by suspending **N0** in an acetone solution of **1** (red) and allowing its diffusion into the hydrophobic cavities for 24 h. During the preparation of **N1** the color of the solid changes from white to blue. This is a consequence of the inclusion of probe **1** into the hydrophobic cavities, through a simple adsorption process, which transformed the red pyrylium stilbene **1** into the blue quinone **2** (formed by the spontaneous deprotonation of probe **1**). By thermogravimetric and elemental analysis, a content of 0.038 mmol of **2** per g SiO_2 in the final **N1** sensing material was determined.

To characterize this red-to-blue color change, a solution of probe **1** in acetonitrile was reacted with 1,8-diazabicyclo-[5.4.0]undec-7-ene (DBU, a non-nucleophilic base) to give an immediate color modulation from red to blue (attributed to **2**, see the Supporting Information). This final blue color was the same as that observed in the sensing **N1** nanoparticles. Moreover, this color transformation went along with changes in the ^{1}H NMR spectrum: the signals of the double bond protons (H_a and H_b) of **1** showed significant upfield shifts with a reduction of the coupling constant (from 16 to 12 Hz) upon addition of DBU to give **2**. Moreover, the hydroxy proton signal of **1** centered at 10.8 ppm disappeared.

The nanoparticles **N0** and **N1** were characterized by standard procedures. Powder X-ray diffraction (PXRD) of as-synthesized siliceous MCM-41 (see the Supporting Information) shows four low-angle reflections typical of a hexagonal array that can be indexed as (100), (110), (200), and (210) Bragg peaks. The PXRD patterns of **N0** and **N1** (see also the Supporting Information) clearly preserve the reflections (100), (110), and (200), thereby evidencing that the surface functionalization and the further loading process with **1** did not damage the mesoporous scaffold. The presence of the mesoporous structure in the starting MCM-41 samples, hydrophobic nanoparticles **N0**, and final sensory material **N1** was also observed by using TEM analysis (see the Supporting Information).

To further explore different formats and to potentially enhance applicability of **N1**, the nanoparticles were included (as a coating) in a rigid monolith with the aim to design ready- and simple-to-use dipsticks for the rapid "in situ" chromofluorimetric screening of sulfite. In particular, a ceramic foam monolith was selected because of its trimodal hierarchical pore system with a high external surface, good mechanical properties, and the possibility to achieve a high degree of coverage with silica nanoparticles.[26]

The ceramic foam monolith was prepared through the replication of commercially available and inexpensive polyurethane foam with a ceramic slip. Then, the surface area of the ceramic foam was activated by using an alkaline-hydrothermal treatment. After the activation process, the coating of the monolith with MCM-41 was carried out by succesive impregnation cycles (4 times) in water suspensions of the nanoparticles followed by a soft thermal treatment. Then, the MCM-41-coated ceramic foam was hydrophobized, thereby yielding the monolith **M0**. Finally, their pores were loaded with derivative **1** resulting in the final blue ceramic foam sensing monolith **M1** (see Figure 1).

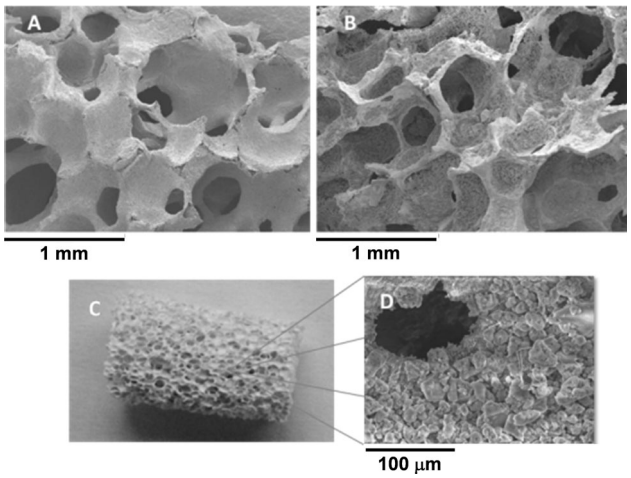

Figure 1. SEM images of A) the ceramic foam before coating and B) after four impregnation cycles with MCM-41 nanoparticles. C) Monolith **M1** and D) SEM image of **M1** macropores.

A preliminary study demonstrated that aqueous solutions of sulfite in the presence of **N1** or **M1** were able to change the color of the solids from blue to pale yellow and at the same time the solids became fluorescent. The pH dependence of color stability of **N1** was also evaluated. **N1** nanoparticles were suspended in water at different pH values and the blue color remained in the 6–9 pH range, with an optimum blue color at pH 7.5 (see the Supporting Information for details).

Figure 2 shows the emission behavior of aqueous buffered (HEPES 30 mM, pH 7.5) suspensions of **N1** nanoparticles in

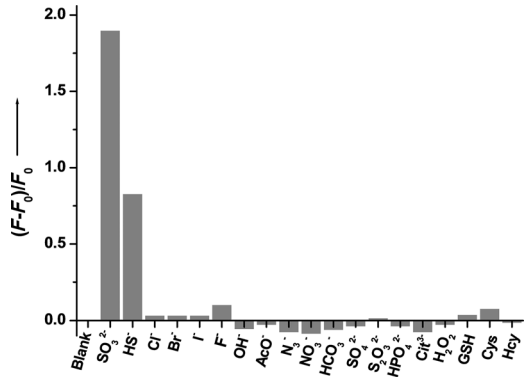

Figure 2. Fluorescence intensity at 460 nm ($\lambda_{ex}=355$ nm) of **N1** nanoparticles in HEPES buffer (30 mM at pH 7.5) in the presence of 10 equivalents of selected anions, biological thiols, and oxidants. Hcy = homocysteine, GSH = glutathione, Cys = cysteine.

the absence and in the presence of selected anions (HS^-, Cl^-, Br^-, I^-, F^-, AcO^-, N_3^-, NO_3^-, HCO_3^-, SO_4^{2-}, SO_3^{2-}, $S_2O_3^{2-}$, HPO_4^{2-}, and citrate), biological thiols (Cys, Hcy, and GSH) and oxidants (H_2O_2). In a typical experiment **N1** (5 mg) was suspended in buffered water (200 μL) containing the corresponding analyte. Then the solid was isolated by centrifugation and the fluorescence at 460 nm ($\lambda_{ex}=355$ nm) was measured. The addition of sulfite anions induced a selective enhancement of the emission (Figure 2) with a concomitant visible color change of the solid from blue to pale-yellow (see the Supporting Information). The HS^- anion also induced the appearance of the fluorescence band at 460 nm, but of less intensity. Remarkably, the addition of the other selected analytes induced negligible changes in the emission of **N1** nanoparticles. The same selective chromofluorogenic response was observed when using the blue ceramic foam monolith **M1** (data not shown).

The change in color and in emission of **2** upon addition of sulfite anions is ascribed to a 1,6-conjugated addition reaction, which yielded the phenol **3** (Scheme 1). This addition was confirmed by NMR experiments (Figure 3)

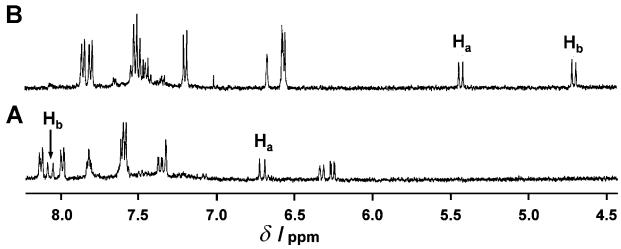

Figure 3. ^{1}H NMR spectra of **2** (A) and **3** (B, obtained upon addition of an excess of sulfite to probe **2**) in [D_6]DMSO.

carried out with quinone **2** (obtained upon deprotonation of **1** with DBU). As shown in Figure 3, the most remarkable signals of quinone **2** are two doublets centered at 8.1 (proton H_b in Scheme 1) and at 6.7 ppm (proton H_a in Scheme 1). Addition of sulfite to **2** induced a marked upfield shift of both H_a and H_b protons to 5.45 (H_a) and 4.65 ppm (H_b) attributed to a loss of aromatic character upon reaction with sulfite anion. HSQC studies (see the Supporting Information) indicated the existence of a clear correlation between proton H_b and a benzylic carbon (at 63.4 ppm) and also between proton H_a and an olefinic carbon (at 116.8 ppm).

The selective response toward sulfite, shown by **2** when incorporated in **N1** nanoparticles, is ascribed to the preferential inclusion of sulfite into the highly hydrophobic pockets in **N1**, which favors the 1,6-conjugated addition reaction. The more hydrophilic HS^- anion was partially included in the hydrophobic cavities, whereas nucleophilic biological thiols (such as Cys, Hcy, and GSH) are too polar and too large to be internalized in the porous network of **N1** nanoparticles. In fact parallel assays carried out using DMSO solutions of **2** demonstrated that **2** is poorly selective and reacted similarly with different nucleophiles such as sulfite, sulfide, GSH, Cys, and Hcy.

Having assessed the selective response of **N1** nanoparticle suspensions to sulfite anions, the sensitivity of the probe was studied by monitoring the emission changes of aqueous buffered (HEPES 30 mM, pH 7.5) suspensions of **N1** nanoparticles upon addition of increasing quantities of sulfite. Increasing the concentration resulted in a progressive and immediate enhancement of fluorescence intensity at 460 nm (Figure 4). From these studies, a remarkable limit of detection (LOD) of 8 μM (0.32 ppm) was calculated. Besides, **N1**

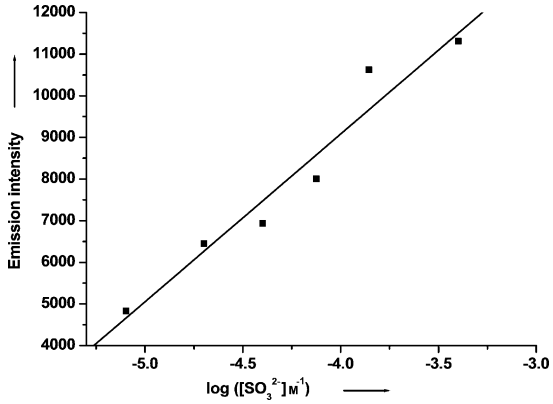

Figure 4. Emission intensity at 460 nm (λ_{ex} = 355 nm) of buffered (HEPES 30 mM, pH 7.5) suspensions of **N1** nanoparticles upon addition of increasing quantities of sulfite.

presents an accurate sensitivity for its potential application in food and in environmental analysis, based on both U.S.A.[6–7] and E.U.[1] standards.

Based on this promising proof-of-principle and taking into account the favorable spectroscopic response of **N1** and **M1**, we explored the possibility of using these materials for the detection of sulfite in complex real samples. In particular we selected sulfite-free red wine that was bleached by simple addition of active carbon and spiked with 20 ppm of sulfite. Then, **M1** monolith was dipped in the doped wine samples and a remarkable and immediate color change from blue to pale yellow was observed (Figure 5 A), whereas when the

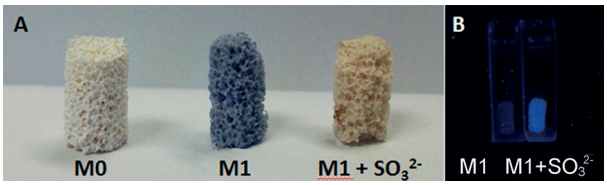

Figure 5. A) Photograph showing the **M0** and **M1** monoliths before (blue) and after (yellow) their reaction with bleached red wine containing 20 ppm of sulfite. B) Fluorescence response under UV irradiation (355 nm).

same material was used in bleached sulfite-free red wine no color change was found. The chromogenic response (visible to the naked eye) was accompanied by a clear emission enhancement (under irradiation with 355 nm UV light) as it can be seen in Figure 5 B.

In an additional experiment the same sulfite-free wine sample was spiked with a known amount of sulfite (6.0 ppm)[27] and the solid **N1** was used to determine sulfite concentration using the well-known standard addition method. In a typical experiment, **N1** nanoparticles (5 mg) were suspended in the bleached wine (200 μL); then increasing volumes of a standard sulfite solution were added and the emission intensity at 460 nm (λ_{ex} = 355 nm) of the samples was measured. By using this procedure a concentration of 5.6 ppm of sulfite was determined (88 % of recovery).

In summary, we have reported here a sensing hybrid material (**N1**) for the simple chromofluorogenic detection of sulfite anions in pure water. The hybrid material was based in MCM-41 mesoporous nanoparticles with hydrophobic cavities able to encompass the chromofluorogenic probe **2**. Of all the anions tested, only sulfite was able to induce a remarkable color change (from blue to pale yellow) with a high emission enhancement. The sulfite detection was selective and sensitive with a limit of detection of 0.32 ppm. In addition, **N1** nanoparticles and **M1** monolith were used for sulfite detection in a complex matrix such as wine. Especially the use of systems such as **M1** opens the possibility of sensing sulfite with the naked eye by using a simple dipstick assay, which may find applications in food and environmental analysis. Moreover the study also demonstrated that the inclusion of chromofluorogenic probes into hydrophobic biomimetic cavities of mesoporous supports is a very simple and promising approach to design sensing materials for anions able to display sensing features in pure water.

Received: July 31, 2013
Revised: September 26, 2013
Published online: November 7, 2013

Keywords: food analysis · mesoporous nanoparticles · organic–inorganic hybrid materials · sensors · sulfite

[1] Council Directive 95/2/EC of the European Parliament and of the Council of 20 February 1995 on food additives other than colors and sweeteners, *Official Journal of the European Communities* L 61, 18.3.1995, pp. 1–53.
[2] a) H. Vally, N. L. A. Misso, V. Madan, *Clin. Exp. Allergy* **2009**, *39*, 1643–1651; b) H. Niknahad, P. J. O'Brien, *Chem.-Biol. Interact.* **2008**, *174*, 147–154.
[3] a) T. Oliphant, A. Mitra, M. Wilkinson, *Contact Dermatitis* **2012**, *66*, 128–130; b) P. García-Ortega, E. Scorza, A. Teniente, *Clin. Exp. Allergy* **2010**, *40*, 688–690.
[4] a) H. Vally, P. J. Thompson, N. L. A. Misso, *Clin. Exp. Allergy* **2007**, *37*, 1062–1066; b) R. K. Bush, S. L. Taylor, K. Holden, J. A. Nordlee, W. W. Busse, *Am. J. Med.* **1986**, *81*, 816–820; c) D. D. Stevenson, R. A. Simon, *J. Allergy Clin. Immunol.* **1981**, *68*, 26–32.
[5] S. Iwasawa, Y. Kikuchi, Y. Nishiwaki, M. Nakano, T. Michikawa, T. Tsuboi, S. Tanaka, T. Uemura, A. Ishigami, H. Nakashima, T. Takebayashi, M. Adachi, A. Morikawa, K. Maruyama, S. Kudo, I. Uchiyama, K. Omae, *J. Occup. Health* **2009**, *51*, 38–47.
[6] W. J. FAO in *WHO food additives series, 60* (Ed.: World Health Organization), Geneva, **2009**.
[7] USEPA, (Ed.: EPA), Virginia, USA, **2007**.
[8] a) X. Shi, *J. Inorg. Biochem.* **1994**, *56*, 155–165; b) J. H. Karchmer, J. W. Dunahoe, *Anal. Chem.* **1948**, *20*, 915–919.
[9] a) G. Li, N. Sang, *Ecotoxicol. Environ. Saf.* **2009**, *72*, 236–241; b) J. Li, R. Li, Z. Meng, *Eur. J. Pharmacol.* **2010**, *645*, 143–150; c) P. J. T. H. Vally, *Thorax* **2001**, *56*, 763–769; d) Y. Y. N. Sang, H. Li, L. Hou, M. Han, G. Li, *Toxicol. Sci.* **2010**, *114*, 226–236.
[10] a) R. Keil, R. Hampp, H. Ziegler, *Anal. Chem.* **1989**, *61*, 1755–1758; b) D. Huang, B. Xu, J. Tang, J. Luo, L. Chen, L. Yang, Z. Yang, S. Bi, *Anal. Methods* **2010**, *2*, 154–158.
[11] a) M. S. Abdel-Latif, *Anal. Lett.* **1994**, *27*, 2601–2614; b) Y. Li, M. Zhao, *Food Control* **2006**, *17*, 975–980; c) J. E. Haskins, H. Kendall, R. B. Baird, *Water Res.* **1984**, *18*, 751–753.
[12] a) K. Akasaka, H. Matsuda, H. Ohrui, H. Meguro, T. Suzuki, *Agric. Biol. Chem.* **1990**, *54*, 501–504; b) L. Pizzoferrato, G.

Di Lullo, E. Quattrucci, *Food Chem.* **1998**, *63*, 275 – 279; c) R. F. McFeeters, A. O. Barish, *J. Agric. Food Chem.* **2003**, *51*, 1513 – 1517; d) H. J. Kim, *J. Assoc. Off. Anal. Chem.* **1990**, *73*, 216 – 222.

[13] a) Z. Daunoravicius, A. Padarauskas, *Electrophoresis* **2002**, *23*, 2439 – 2444; b) T. Fazio, C. R. Warner, *Food Addit. Contam.* **1990**, *7*, 433 – 454; c) G. Jankovskiene, Z. Daunoravicius, A. Padarauskas, *J. Chromatogr. A* **2001**, *934*, 67 – 73.

[14] a) M. O. Health, *Analyst* **1927**, *52*, 343 – 344; b) N. T. K. Thanh, L. G. Decnop-Weever, W. T. Kok, *Fresenius J. Anal. Chem.* **1994**, *349*, 469 – 472; c) J. B. Thompson, E. Toy, *Ind. Eng. Chem. Anal. Ed.* **1945**, *17*, 612 – 615.

[15] a) L. E. Santos-Figueroa, M. E. Moragues, E. Climent, A. Agostini, R. Martinez-Manez, F. Sancenon, *Chem. Soc. Rev.* **2013**, *42*, 3489 – 3613; b) N. R. Song, J. H. Moon, J. Choi, E. J. Jun, Y. Kim, S. J. Kim, J. Y. Lee, J. Yoon, *Chem. Sci.* **2013**, *4*, 1765 – 1771.

[16] a) G. J. Mohr, *Chem. Commun.* **2002**, 2646 – 2647; b) K. Chen, Y. Guo, Z. Lu, B. Yang, Z. Shi, *Chin. J. Chem.* **2010**, *28*, 55 – 60; c) X.-F. Yang, M. Zhao, G. Wang, *Sens. Actuators B* **2011**, *152*, 8 – 13; d) Y.-Q. Sun, P. Wang, J. Liu, J. Zhang, W. Guo, *Analyst* **2012**, *137*, 3430 – 3433; e) Y. Yang, F. Huo, J. Zhang, Z. Xie, J. Chao, C. Yin, H. Tong, D. Liu, S. Jin, F. Cheng, X. Yan, *Sens. Actuators B* **2012**, *166 – 167*, 665 – 670; f) C. Yu, M. Luo, F. Zeng, S. Wu, *Anal. Methods* **2012**, *4*, 2638 – 2640; g) X. Cheng, H. Jia, J. Feng, J. Qin, Z. Li, *Sens. Actuators B* **2013**, *184*, 274 – 280; h) G. Wang, H. Qi, X.-F. Yang, *Luminescence* **2013**, *28*, 97 – 101.

[17] a) X. Gu, C. Liu, Y.-C. Zhu, Y.-Z. Zhu, *J. Agric. Food Chem.* **2011**, *59*, 11935 – 11939; b) M. G. Choi, J. Hwang, S. Eor, S.-K. Chang, *Org. Lett.* **2010**, *12*, 5624 – 5627; c) S. Chen, P. Hou, J. Wang, X. Song, *RSC Adv.* **2012**, *2*, 10869 – 10873.

[18] a) M.-Y. Wu, T. He, K. Li, M.-B. Wu, Z. Huang, X.-Q. Yu, *Analyst* **2013**, *138*, 3018 – 3025; b) Y.-Q. Sun, J. Liu, J. Zhang, T. Yang, W. Guo, *Chem. Commun.* **2013**, *49*, 2637 – 2639.

[19] a) J. Xu, K. Liu, D. Di, S. Shao, Y. Guo, *Inorg. Chem. Commun.* **2007**, *10*, 681 – 684; b) R. C. Rodríguez-Díaz, M. P. Aguilar-Caballos, A. Gómez-Hens, *J. Agric. Food Chem.* **2004**, *52*, 7777 – 7781; c) Y. Sun, C. Zhong, R. Gong, H. Mu, E. Fu, *J. Org. Chem.* **2009**, *74*, 7943 – 7946.

[20] A. Zhu, Q. Qu, X. Shao, B. Kong, Y. Tian, *Angew. Chem.* **2012**, *124*, 7297 – 7301; *Angew. Chem. Int. Ed.* **2012**, *51*, 7185 – 7189.

[21] a) J. Zhang, X. Xu, X. Yang, *Analyst* **2012**, *137*, 3437 – 3440; b) J. Zhang, Y. Yuan, X. Wang, X. Yang, *Anal. Methods* **2012**, *4*, 1616 – 1618.

[22] H. Xie, F. Zeng, C. Yu, S. Wu, *Polym. Chem.* **2013**, *14*, 5416 – 5424.

[23] C. Pundir, R. Rawal, *Anal. Bioanal. Chem.* **2013**, *405*, 3049 – 3062.

[24] a) E. Climent, R. Martínez-Máñez, F. Sancenón, M. D. Marcos, J. Soto, A. Maquieira, P. Amorós, *Angew. Chem.* **2010**, *122*, 7439 – 7441; *Angew. Chem. Int. Ed.* **2010**, *49*, 7281 – 7283; b) C. Coll, A. Bernardos, R. Martínez-Máñez, F. Sancenón, *Acc. Chem. Res.* **2013**, *46*, 339 – 349.

[25] a) G. Kickelbick, *Angew. Chem.* **2004**, *116*, 3164 – 3166; *Angew. Chem. Int. Ed.* **2004**, *43*, 3102 – 3104; b) A. Stein, *Adv. Mater.* **2003**, *15*, 763 – 775; c) A. P. Wight, M. E. Davis, *Chem. Rev.* **2002**, *102*, 3589 – 3614; d) S.-H. Wu, C.-Y. Mou, H.-P. Lin, *Chem. Soc. Rev.* **2013**, *42*, 3862 – 3875; e) F. Tang, L. Li, D. Chen, *Adv. Mater.* **2012**, *24*, 1504 – 1534; f) K. Ariga, A. Vinu, Y. Yamauchi, Q. Ji, J. P. Hill, *Bull. Chem. Soc. Jpn.* **2012**, *85*, 1 – 32; g) P. Innocenzi, L. Malfatti, *Chem. Soc. Rev.* **2013**, *42*, 4198 – 4216.

[26] a) J. El Haskouri, D. O. d. Zarate, C. Guillem, J. Latorre, M. Caldes, A. Beltran, D. Beltran, A. B. Descalzo, G. Rodriguez-Lopez, R. Martinez-Manez, M. D. Marcos, P. Amoros, *Chem. Commun.* **2002**, 330 – 331; b) L. Huerta, J. El Haskouri, D. Vie, M. Comes, J. Latorre, C. Guillem, M. D. Marcos, R. Martínez-Mañez, A. Beltrán, D. Beltrán, P. Amorós, *Chem. Mater.* **2007**, *19*, 1082 – 1088.

[27] Concentrations of less that 10 ppm were selected because this is the maximum concentration limit allowed for red wine that is sold as SO_3^{2-} free wine according to E.U. regulations.

